Journal of Physics: Conference Series **3177** (2026) 012108 doi:10.1088/1742-6596/3177/1/012108

Crystalline toplayer concept for absorption reduction

D Diksha[1,2], I El Ouedghiri-Idrissi[1,2], L Massaro [1,2], A Amato[1,2], J Woehler [1,2], I W Martin[4], J Steinlechner[1,2,4]

[1] Maastricht University, Minderbroedersberg 4-6, 6211 LK Maastricht, The Netherlands
[2] Nikhef, Science Park 105, 1098 XG Amsterdam, The Netherlands
[4] SUPA, School of Physics and Astronomy, University of Glasgow, Glasgow, G12 8QQ, Scotland

E-mail: d.diksha@maastrichtuniversity.nl

E-mail: jessica.steinlechner@maastrichtuniversity.nl

Abstract.

The performance of gravitational-wave detectors relies critically on highly-reflective mirror coatings with minimal thermal noise and optical absorption. Amorphous silicon and silicon nitride are promising low-noise materials for future, cryogenically operated detectors, but their optical absorption remains too high. Besides material improvement, absorption mitigation strategies include design optimization. In this article, we discuss the concept of using a crystalline toplayer as part of an otherwise amorphous coating and the improvement achievable with such a coating design. Furthermore, we present analysis of a crystalline layer produced via high energy oxygen ion implantation.

1 Background

One of the most groundbreaking discoveries in recent decades has been the detection of gravitational waves from sources such as black hole mergers and binary neutron stars [1–3] by Advanced LIGO (aLIGO) [4] and Advanced Virgo [5]. Research for the next generation of detectors such as the Einstein Telescope (ET) [6] is ongoing, with the aim of a ten times improved sensitivity compared to current detectors.

One of the main factors limiting the detectors' sensitivity is thermal noise of their highly-reflective mirror coatings, which are made of alternating layers of two materials with high and low refractive index n. Figure 1(a) shows the design sensitivity of aLIGO (gray curve), which is limited by several noise sources [7]. The red line shows the contribution of coating thermal noise to this overall noise level.

Coating thermal noise is proportional to the square roots of the mirror temperature T, the coating thickness d, and the coating mechanical loss ϕ, and inversely proportional to the square root of the detection frequency f and to the the laser beam diameter w on the mirror [8, 9],

$$X(f,T) \propto \sqrt{\frac{T}{f}\frac{d}{w^2}\phi}\,. \tag{1}$$

To overcome the thermal noise limitation, future detectors such as ET are planned to operate at cryogenic temperatures [6], a technology already adopted by KAGRA [10]. Furthermore, larger mirrors, and consequently laser beams, will be used. Due to a change of substrate material, the laser wavelength will have to be increased from 1064 nm (used in current detectors) to 1550 nm or 2000 nm, resulting in slightly thicker coatings scaling with the wavelength. The mechanical loss ϕ is a strongly temperature dependent material property with current coating materials, TiO_2:Ta_2O_5 and SiO_2 [12], showing loss

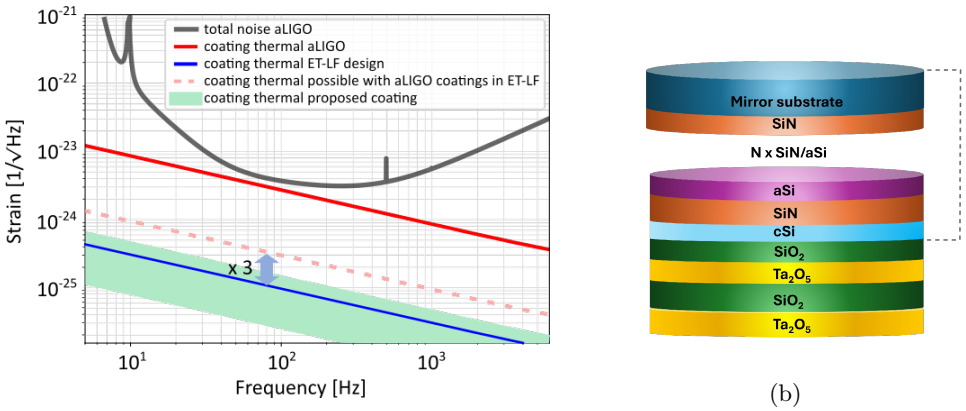

(a) (b)

Figure 1: (a) aLIGO design sensitivity (gray curve) and coating thermal noise (red, solid line) - adapted from [11]. Dashed, light red line: Coating thermal noise in ET when using current coatings at 10 K and 2000 nm. Blue, solid line: Coating thermal noise required for ET. Green-shaded area: Thermal noise of the coating discussed in this article. (b) Schematic of a possible coating stack incorporating one crystalline silicon (cSi) layer, but otherwise made of amorphous layers.

peaks at cryogenic temperatures [13–15], partly counteracting the benefit from cooling. The resulting coating thermal noise achievable with current coatings when used in the ET at 10 K and 2000 nm – to discuss the slightly higher-noise scenario based on a thicker coating at 2000 nm than at 1550 nm – is shown by the dashed, light red line in Fig. 1(a). This level exceeds the ET design (solid, blue line) [6] by approximately a factor of three, despite cooling. Consequently, new coating solutions are required.

Amorphous silicon (aSi) and silicon nitride (SiN) are promising coating materials, both showing very low mechanical loss at low temperatures [16]. aSi would serve as the high-n material [17, 18], and SiN as the low-n material [19, 20]. For a highly-reflective end test-mass mirrors (ETM), used in a gravitational-wave detector (GWD), about 11 bilayers of aSi/SiN would be required, and about 6 bilayers for the lower-reflective input test-mass mirrors (ITM). With such coatings, a thermal noise performance at the lower boundary of the green-shaded area in Fig. 1(a) would be achievable.

Low optical absorption of the order of 1 – 5 ppm is another requirement of coatings used in GWDs. However, both aSi and SiN exhibit too high absorption, expected to result in ≈ 27 ppm at 2000 nm and low temperatures, and even higher at 1550 nm [21]. Ways to further reduce the absorption include

- further research into optimizing the coating materials [22, 23],
- using a multimaterial design [24–26],
- and adding a crystalline toplayer into the coating stack [27].

In this article, we will introduce a specific crystalline toplayer design, based on aSi and SiN layers, and discuss the production and analysis of the crystalline layer.

2 The Crystalline Toplayer concept

The availability of materials which exhibit low optical absorption and low mechanical loss at low temperatures is very limited, but a variety of materials show one or the other. Based on this, the concept of multimaterial coatings was developed [24–26]. Such coatings use materials with low optical absorption in the first layers of the highly-reflective stack (seen from the direction of the reflected beam), where the laser light power, and consequently the absorbed light fraction, is high. In the lower layers, where the light field is low, materials with higher optical absorption, but instead low mechanical loss can be used.

It was shown previously that employing even just one high-n layer at the top of the coating stack can substantially decrease the power transmission into the lower coating layers, thereby reducing the absorption [27]. The thickness of such a layer has to be a quarter of a wavelength in optical thickness, i.e. $2000\,\text{nm}/(4 \times n)$. Crystalline silicon, with $n \approx 3.5$ at 1550 – 2000 nm [28], shows very low optical absorption and mechanical loss [29, 30], negligible for a layer of only ≈ 140 nm.

A mono-crystalline layer, required to achieve low optical scattering, cannot be grown on an otherwise amorphous coating. However, the industrially well-established silicon-on-insulator (SOI) technology can

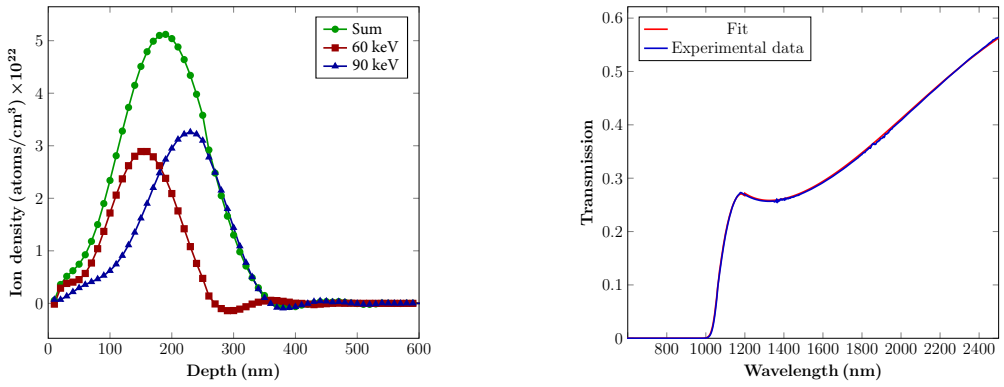

(a) (b)

Figure 2: (a) Simulated ion density depth profile resulting from two implantation energies used to form a layer. (b) Transmission spectrum of the implanted sample (blue) and fit based on optical models (red).

potentially provide such a layer. An SOI wafer consists of a crystalline silicon carrier several hundred microns thick, from which another crystalline silicon layer, which can be as thin as a few 10 to 100 nm, is separated by a silicon dioxide layer [31, 32].

The production steps of a highly-reflective amorphous coating with a crystalline toplayer would be:

- deposit an amorphous aSi/SiN multilayer coating on the thin silicon layer of an SOI wafer, starting and ending with an SiN layer,
- bond the wafer 'upside down' to the mirror substrate with the amorphous layers facing the substrate,
- remove first the carrier wafer, followed by removing the silicon dioxide layer which serves as an etch stop, in two separate etching steps.

Figure 1(b) shows the resulting system, marked by the dashed bracket: The dark blue layer at the top represents the mirror substrate, followed by several bilayers of SiN and aSi. The system is concluded by a crystalline-silicon toplayer, shown in light blue.

The absorption of the whole coating is reduced from initially ≈ 27 ppm to ≈ 13.5 ppm as the crystalline layer reflects $\approx 50\,\%$ of laser power before it reaches the amorphous layers underneath. This twofold absorption reduction is achieved without adding to the coating's thermal noise, which is still represented by the lower boundary of the green-shared area in Fig. 1(a).

Further absorption reduction can be achieved by adding additional bilayers of SiO_2 and Ta_2O_5 – with or without TiO_2 doping – on top of the crystalline layer as indicated in Fig. 1(b). With every bilayer, the coating absorption is reduced by another factor of ≈ 2, reaching < 5 ppm after two bilayers (shown in Fig. 1(b)) and < 1 ppm after four bilayers. However, these bilayers add substantially to the overall coating thermal noise: A coating with four bilayers of SiO_2 and Ta_2O_5 is represented by the upper boundary of the green-shaded area in Fig. 1(a). Some, or all, of the high-loss SiO_2 and Ta_2O_5 layers may become unnecessary, moving thermal noise from the upper limit downwards, by reducing the absorption aSi and/or SiN. Research to improve these materials is ongoing.

3 Toplayer production by ion implantation

A variety of high-quality off-the-shelf SOI wafers, usually produced for the semi-conductor industry, are commercially available. However, for application in mirror coatings, non-standard layer thickness and high-purity silicon are required. Therefore, a first silicon-on-insulator prototype was produced in situ through oxygen ion implantation [] for application as silicon toplayer in coatings.

In this process, oxygen ions were implanted into a silicon wafer of 1 mm thickness at high energies. To create the BOX (i.e. buried oxide) layer with oxygen rich location in the silicon, two energies were used for the oxygen ions, 60 keV and 90 keV. The ion dose for both energies was maintained at 3.8×10^{17}, calculated using the SRIM[1] software. A simulation of the desired implanted profile is shown in Fig. 2(a).

To characterize the sample, transmission spectra were obtained using a Cary 5000 spectrophotometer [34] in the range of 175 nm to 2500 nm, with a step size of 1 nm. The transmission spectra were analyzed using SCOUT [35] to extract the optical parameters of the layers. In the first step, a dielectric

model of crystalline silicon was obtained using an identical wafer with no ions implanted. To form the dielectric model, two models were used at different spectral ranges in combination; first we used the model from the study presented in [36] from 250 nm to 1200 nm, and from 1200 nm to 2500 nm, we used the Cauchy model [37], keeping the temperature conditions at 295 K. Then, without changing the silicon properties modeled, a SiO_2 thin layer was stacked on top, using the Sellmeier model [37]. In a final step, a crystalline thin layer was added, using the properties for crystalline silicon initially obtained from the bare wafer. The crystalline toplayer of the SOI was optically analyzed to be 83 nm thick with $n = 3.40$ at 2000 nm, separated from the carrier wafer by the implanted SiO_2 layer layer of 210 nm thickness and $n = 1.84$. Figure 2(b) shows the measured transmission data (blue) and the fitted model (red). The layer thicknesses obtained are in agreement with the SRIM simulation shown in Fig. 2(b). Deviations of n from standard values for cSi and SiO_2 likely result from the non-sharp layer profile and from the fact that heat treatment may be required to further support the formation of SiO_2.

4 Conclusions

A coating made of aSi/SiN was previously suggested to meet the thermal noise requirements of future cryogenic GWDs such as ET [6, 21]. To also meet the absorption requirement, we suggest adding a high refractive index crystalline silicon layer on top of the stack. With ≈ 13.5 ppm, the resulting coating still exceeds the absorption requirements which are of the order $1 - 5$ ppm. To meet this requirement, we suggest further work on absorption reduction of aSi and SiN, combined with a multimaterial design [24–26], posing an absorption and thermal noise trade-off.

Furthermore, we present a production option for the crystalline silicon layer by employing oxygen ion implantation. The main result from the production and analysis of this first prototype is that we obtained a model reproducing the optical properties of the layer system, confirming consistency with the SRIM model. This paves the way for further sample production for the implementation of the crystalline toplayer concept.

5 Acknowledgments

This work is supported by ERC grant MIRRORS, Project No. 101040572, funded by the European Union. Views and opinions expressed are however those of the authors only and do not necessarily reflect those of the European Union or the European Research Council Executive Agency. Neither the European Union nor the granting authority can be held responsible for them. We acknowledge support by ETpathfinder (Interreg Vlaanderen-Nederland), E-TEST (Interreg Euregio Meuse-Rhine), the Dutch Research Council (NWO) Project No. VI.Vidi.203.062 and OCENW.KLEIN.560, the Province of Limburg, and STFC for support via ST/V005634/1 and ST/X004740/1. We would like to thank François Schiettekatte and Martin Chicoine for valuable discussions.

This paper has LIGO Document number LIGO-P2500535.

References

[1] Abbott B P, Abbott R, Abbott T D, Abernathy M R, Acernese F, Ackley K, Adams C, Adams T, Addesso P, Adhikari R X *et al.* (LIGO Scientific Collaboration and Virgo Collaboration) 2016 *Phys. Rev. Lett.* **116**(6) 061102 URL `https://link.aps.org/doi/10.1103/PhysRevLett.116.061102`

[2] LIGO Scientific Collaboration and Virgo Collaboration 2021 *Phys. Rev. X* **11**(2) 021053 URL `https://link.aps.org/doi/10.1103/PhysRevX.11.021053`

[3] Abbott R, Abbott T D, Acernese F, Ackley K, Adams C, Adhikari N, Adhikari R X, Adya V B, Affeldt C *et al.* 2021 GWTC-3: Compact binary coalescences observed by LIGO and Virgo during the second part of the third observing run (*Preprint* `2111.03606`) URL `https://arxiv.org/abs/2111.03606v2`

[4] Aasi J, Abbott B, Abbott R, Abbott T, Abernathy M, Ackley K, Adams C, Adams T, Addesso P, Adhikari R *et al.* 2015 *Classical and Quantum Gravity* **32**

[5] Acernese F, Agathos M, Agatsuma K, Aisa D, Allemandou N, Allocca A, Amarni J, Astone P, Balestri G *et al.* 2015 *Classical and Quantum Gravity* **32**

[6] ET steering committee 2020 *ET-0007B-20* URL `https://apps.et-gw.eu/tds/?content=3&r=17245`

[7] Buikema A, Cahillane C, Mansell G L, Blair C D, Abbott R, Adams C, Adhikari R X, Ananyeva A, Appert S, Arai K *et al.* 2020 *Phys. Rev. D* **102**(6) 062003 URL https://link.aps.org/doi/10.1103/PhysRevD.102.062003

[8] Harry G M, Armandula H, Black E, Crooks D R M, Cagnoli G, Hough J, Murray P, Reid S, Rowan S, Sneddon P, Fejer M M, Route R and Penn S D 2006 *Appl. Opt.* **45** 1569–1574 URL https://opg.optica.org/ao/abstract.cfm?URI=ao-45-7-1569

[9] Hong T, Yang H, Gustafson E K, Adhikari R X and Chen Y 2013 *Phys. Rev. D* **87**(8) 082001 URL https://link.aps.org/doi/10.1103/PhysRevD.87.082001

[10] Akutsu T, Ando M, Arai K, Arai Y, Araki S, Araya A, Aritomi N, Aso Y, Bae S, Bae Y *et al.* 2020 *Progress of Theoretical and Experimental Physics* **2021** 05A101 URL https://doi.org/10.1093/ptep/ptaa125

[11] Lisa Barsotti Peter Fritschel M E S G 2018 *LIGO Scientific Collaboration technical report* URL https://dcc.ligo.org/LIGO-T1800044/public

[12] Granata M, Amato A, Canepa M, Degallaix J, Forest D, Dolique V, Mereni L, Michel C, Pinard L, Sassolas B, Teillon J and Cagnoli G 2020 *Classical and Quantum Gravity* **37**

[13] Martin I, Armandula H, Comtet C, Fejer M M, Gretarsson A, Harry G, Hough J, Mackowski J M M, MacLaren I, Michel C, Montorio J L, Morgado N, Nawrodt R, Penn S, Reid S, Remillieux A, Route R, Rowan S, Schwarz C, Seidel P, Vodel W and Zimmer A 2008 *Classical and Quantum Gravity* **25** 055005 URL https://doi.org/10.1088/0264-9381/25/5/055005

[14] Martin I W, Chalkley E, Nawrodt R, Armandula H, Bassiri R, Comtet C, Fejer M M, Gretarsson A, Harry G, Heinert D, Hough J, MacLaren I, Michel C, Montorio J L, Morgado N, Penn S, Reid S, Route R, Rowan S, Schwarz C, Seidel P, Vodel W and Woodcraft A L 2009 *Classical and Quantum Gravity* **26** 155012 URL https://doi.org/10.1088/0264-9381/26/15/155012

[15] Martin I W, Bassiri R, Nawrodt R, Fejer M M, Gretarsson A, Gustafson E, Harry G, Hough J, MacLaren I, Penn S, Reid S, Route R, Rowan S, Schwarz C, Seidel P, Scott J and Woodcraft A L 2010 *Classical and Quantum Gravity* **27** 225020 URL https://doi.org/10.1088/0264-9381/27/22/225020

[16] Southworth D R, Barton R A, Verbridge S S, Ilic B, Fefferman A D, Craighead H G and Parpia J M 2009 *Phys. Rev. Lett.* **102**(22) 225503 URL https://link.aps.org/doi/10.1103/PhysRevLett.102.225503

[17] Steinlechner J, Martin I W, Bassiri R, Bell A, Fejer M M, Hough J, Markosyan A, Route R K, Rowan S and Tornasi Z 2016 *Phys. Rev. D* **93**(6) 062005 URL https://link.aps.org/doi/10.1103/PhysRevD.93.062005

[18] Terkowski L, Martin I W, Axmann D, Behrendsen M, Pein F, Bell A, Schnabel R, Bassiri R, Fejer M M, Hough J, Markosyan A, Rowan S and Steinlechner J 2020 *Phys. Rev. Res.* **2**(3) 033308 URL https://link.aps.org/doi/10.1103/PhysRevResearch.2.033308

[19] Amato A, Bazzan M, Cagnoli G, Canepa M, Coulon M, Degallaix J, Demos N, Di Michele A, Evans M, Fabrizi F *et al.* 2025 *Phys. Rev. D* **111**(4) 042003 URL https://link.aps.org/doi/10.1103/PhysRevD.111.042003

[20] Wallace G S, Yaala M B, Tait S C, Vajente G, McCanny T, Clark C, Gibson D, Hough J, Martin I W, Rowan S and Reid S 2024 *Classical and Quantum Gravity* **41** 095005 URL https://dx.doi.org/10.1088/1361-6382/ad35a1

[21] Steinlechner J, Martin I W, Bell A S, Hough J, Fletcher M, Murray P G, Robie R, Rowan S and Schnabel R 2018 *Phys. Rev. Lett.* **120**(26) 263602 URL https://link.aps.org/doi/10.1103/PhysRevLett.120.263602

[22] Tsai D S, Huang Z L, Chang W C and Chao S 2022 *Classical and Quantum Gravity* **39** 15LT01 URL https://dx.doi.org/10.1088/1361-6382/ac79f6

[23] Molina-Ruiz M, Markosyan A, Bassiri R, Fejer M M, Abernathy M, Metcalf T H, Liu X, Vajente G, Ananyeva A and Hellman F 2023 *Phys. Rev. Lett.* **131**(25) 256902 URL https://link.aps.org/doi/10.1103/PhysRevLett.131.256902

[24] Yam W, Gras S and Evans M 2015 *Phys. Rev. D* **91**(4) 042002 URL https://link.aps.org/doi/10.1103/PhysRevD.91.042002

[25] Steinlechner J, Martin I W, Hough J, Krüger C, Rowan S and Schnabel R 2015 *Phys. Rev. D* **91**(4) 042001 URL https://link.aps.org/doi/10.1103/PhysRevD.91.042001

[26] Tait S C, Steinlechner J, Kinley-Hanlon M M, Murray P G, Hough J, McGhee G, Pein F, Rowan S, Schnabel R, Smith C, Terkowski L and Martin I W 2020 *Phys. Rev. Lett.* **125**(1) 011102 URL https://link.aps.org/doi/10.1103/PhysRevLett.125.011102

[27] Steinlechner J and Martin I W 2016 *Phys. Rev. D* **93**(10) 102001 URL https://link.aps.org/doi/10.1103/PhysRevD.93.102001

[28] Li H H 1980 *Journal of Physical and Chemical Reference Data* **9** 561–658 URL https://doi.org/10.1063/1.555624

[29] Keevers M J and Green M A 1995 *Applied Physics Letters* **66** 174–176 URL https://doi.org/10.1063/1.113125

[30] McGuigan D F, Lam C C, Gram R Q, Hoffman A W, Douglass D H and Gutche H W 1978 *J. Low Temp. Phys.* **30** 621–629

[31] Nakashima S and Izumi K 1993 *Journal of Materials Research* **8** 523–534

[32] Ohashi H, Ohura J, Tsukakoshi T and Simbo M 1986 *1986 International Electron Devices Meeting* pp 210–213

[33] Burnham M E and Wilson S R 1985 *Advanced Applications of Ion Implantation* vol 0530 ed Current M I and Sadana D K International Society for Optics and Photonics (SPIE) pp 240 – 250 URL https://doi.org/10.1117/12.946492

[34] Agilent, cary 5000 uv-vis-nir URL https://www.agilent.com/en/product/molecular-spectroscopy/uv-vis-uv-vis-nir-spectroscopy/uv-vis-uv-vis-nir-systems/cary-5000-uv-vis-nir

[35] W.theiss hard- and software URL https://www.wtheiss.com/

[36] Schinke C, Christian Peest P, Schmidt J, Brendel R, Bothe K, Vogt M R, Kröger I, Winter S, Schirmacher A, Lim S, Nguyen H T and MacDonald D 2015 *AIP Advances* **5** 067168 URL https://doi.org/10.1063/1.4923379

[37] Cushman C, Smith N, Kaykhaii M, Podraza N and Linford M 2016 *Vacuum Technology & Coating* **7**